

Wave propagation in periodic nonlinear dielectric superlattices

D. Hennig

Freie Universität Berlin, Fachbereich Physik, Institut für Theoretische Physik, Arnimallee 14, 14195 Berlin, Germany, and Computational Physics Laboratory, Department of Physics, University of North Texas, Denton, Texas 76203

H. Gabriel

Freie Universität Berlin, Fachbereich Physik, Institut für Theoretische Physik, Arnimallee 14, 14195 Berlin, Germany

G. P. Tsironis

Computational Physics Laboratory, Department of Physics, University of North Texas, Denton, Texas 76203, and Research Center of Crete and Physics Department, University of Crete, P. O. Box 1527, Heraklion 71110, Crete, Greece

M. Molina

Computational Physics Laboratory, Department of Physics, University of North Texas, Denton, Texas 76203

(Received 4 March 1994; accepted for publication 1 April 1994)

We investigate wave propagation in a superlattice consistent of dielectric material with a nonlinear Kerr coefficient. We find gaps in the propagating properties of the medium that depend critically on the injected wave power. This property can be used for transmission of information.

Novel phenomena such as photonic band gaps and possible light localization occur when electromagnetic (EM) waves propagate in dielectric superlattices.¹⁻⁶ In an approximation where only the scalar nature of the EM wave is taken into account, wave propagation in a periodic or disordered medium resembles the dynamics of an electron in a crystal lattice. As a result, photonic bands and gaps arise in the periodic lattice case whereas EM wave localization is theoretically possible in the disordered case. In the latter case and when the dielectric medium is one dimensional, Anderson-type optical localization has been predicted.^{1,2} In an ordered dielectric superlattice, on the other hand, photon band gaps have been demonstrated for various realistic configurations.⁵ One issue that has not been widely addressed yet is the possibility of using superlattices with nonlinear dielectric properties and, in particular, the nonlinear Kerr effect, to construct optical devices with desired transmission characteristics.^{2,7} This is the problem we are addressing in the present letter.

We consider the propagation of plane EM waves in the scalar approximation in a one-dimensional continuous linear dielectric medium. In the medium we embed periodically small dielectric regions that have non-negligible third order nonlinear susceptibility $\chi^{(3)}$ (Fig. 1). We will assume for simplicity that the width of the nonlinear dielectric regions is much smaller than the distance between two adjacent ones. We are thus led to a model for a periodic nonlinear superlattice and the propagation of a plane wave injected on one side of the structure can be described through the following nonlinear Kronig-Penney equation:

$$\omega u(z) = -\frac{d^2 u(z)}{dz^2} + \alpha \sum_{n=1}^N \delta(z-n) \times (1 + \lambda |u(z)|^2) u(z). \quad (1)$$

In Eq. (1), u is the complex amplitude of an incoming plane wave with frequency ω along direction z , α is proportional to

the dielectric constant of the dielectric in each superlattice slab and λ is a nonlinear coefficient that incorporates $\chi^{(3)}$ and the input wave power.⁸ The series of equidistant delta functions represent the effect of the periodic nonlinear dielectric medium on the wave propagation. Straightforward manipulations similar to the ones used in the standard linear Kronig-Penney problem lead to the following nonlinear difference equation for $u_j \equiv u(j)^{9-11}$

$$u_{j+1} + u_{j-1} = \left(2 \cos(k) + \alpha (1 + \lambda |u_j|^2) \frac{\sin(k)}{k} \right) u_j, \quad (2)$$

where k is the wave number associated with the frequency $\omega(k) = 2 \cos k$. A local transformation to polar coordinates and a subsequent grouping of pairs of adjacent variables u_{n-1}, u_n turns Eq. (2) to the following two-dimensional map M :¹¹

$$x_{n+1} = \left[2 \cos(k) + \alpha \left(1 + \frac{1}{2} \lambda (W_n + z_n) \right) \frac{\sin(k)}{k} \right] \times (W_n + z_n) - x_n, \quad (3)$$

$$z_{n+1} = z_n - \frac{1}{2} \frac{x_n^2 - x_{n+1}^2}{W_n + z_n}, \quad (4)$$

where $W_n = \sqrt{x_n^2 + z_n^2 + 4J^2}$, $x_n = 2r_n r_{n-1} \cos(\theta_n - \theta_{n-1})$, $z_n = r_n^2 - r_{n-1}^2$ with $u_n = r_n \exp(i\theta_n)$ and J is the conserved current, i.e., $J = 2r_n r_{n-1} \sin(\theta_n - \theta_{n-1})$.

The map M can contain bounded and diverging orbits. The former ones correspond to transmitting waves whereas the latter correspond to waves with amplitude escaping to infinity and hence do not contribute to wave transmission. The structure on the phase plane (x_n, z_n) is organized by a hierarchy of periodic orbits surrounded by quasiperiodic orbits. As the value of λ increases some periodic orbits become unstable leading to stochasticity. This corresponds to passage from a transmitting to a nontransmitting region. In Fig. 2 we show one orbit corresponding to the period-4 Poincaré-

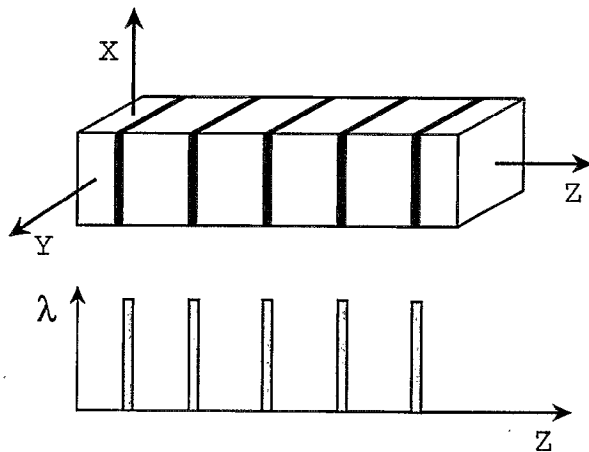


FIG. 1. A periodic dielectric superlattice with nonlinear susceptibility due to the Kerr effect. The dark regions denote the dielectric slabs with nonlinear properties. The periodic value of the nonlinear coefficient λ is approximated by the periodic delta functions.

Birkhoff resonance zone. In Fig. 2(a) the regular periodic orbit surrounding the four fixed points corresponds to wave transmission through the superlattice. In Fig. 2(b) on the other hand, the same trajectory is shown for a larger incident wave amplitude. We observe that a thin chaotic layer has developed that surrounds the separatrix but also some scat-

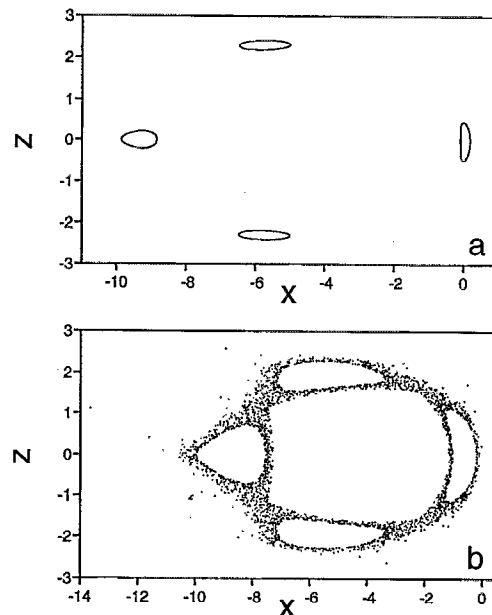


FIG. 2. Orbit of the map corresponding to the period-4 Poincaré-Birkhoff chain. Parameters: $k=4.7$, $\lambda=1$ and the incoming wave intensity $|R_0|$ is in (a) 1.6 and in (b) 1.7. In both (a) and (b) the same trajectory is plotted. We note the chaotic nature of the trajectory in (b) leading to nonpropagating waves.

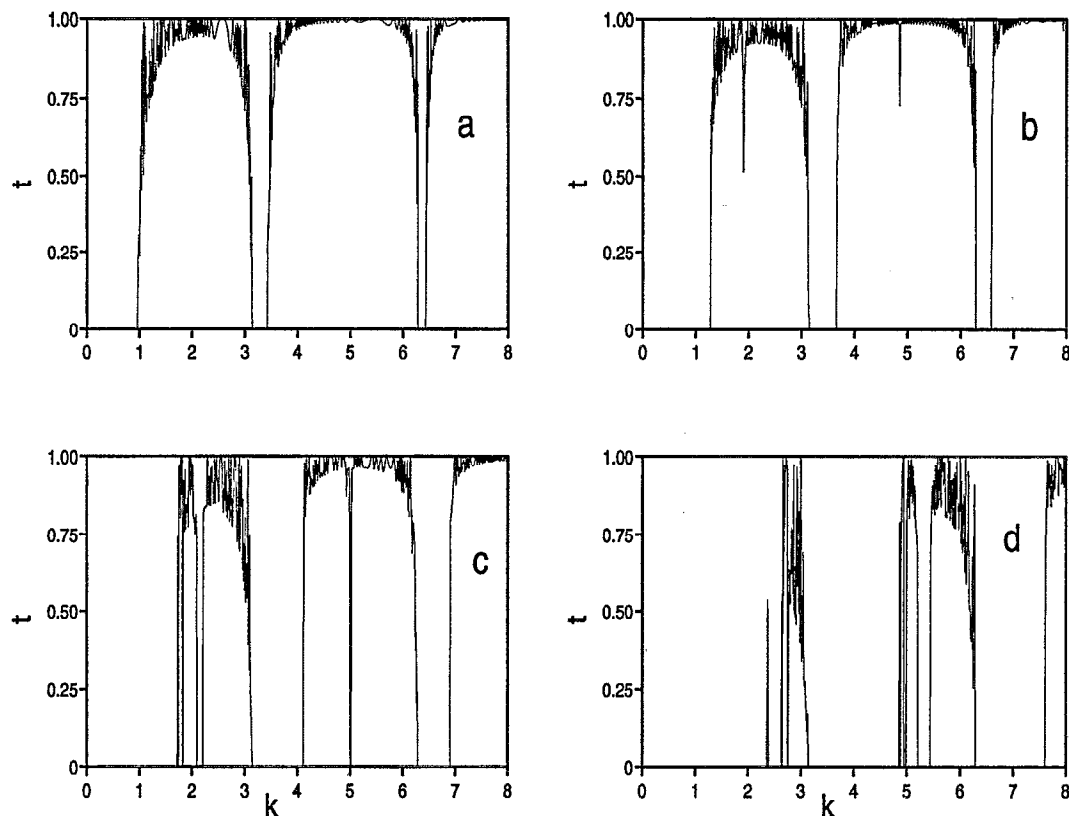


FIG. 3. (a) Transmission coefficient as a function of the wave number k for λ equal to (a) zero (linear case), (b) 0.2, (c) 1.0, and (d) 4.0. The value of the linear coefficient is $\alpha=1$ and the amplitude of the injected wave is taken as unity.

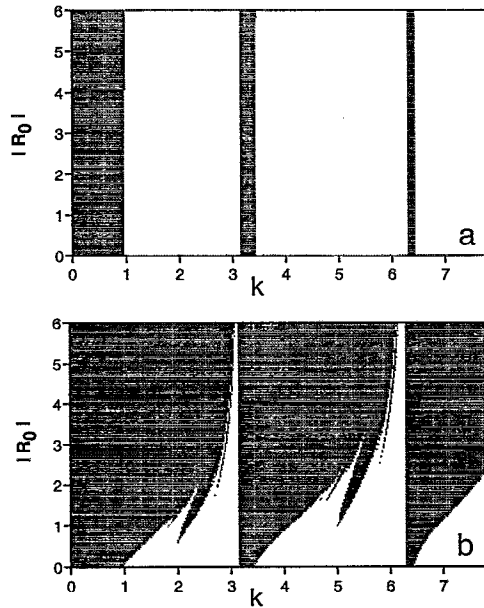


FIG. 4. Amplitude of injected wave R_0 as a function of the wave number k for λ equal to (a) zero (linear case) and (b) 1.0. The value of the linear coefficient is $\alpha=1$. The superlattice has 4000 nonlinear slabs. Transmitting solutions correspond to the blank area whereas diverging solutions are indicated by the hatched area.

tered points escaping to larger z values are visible. This trajectory corresponds to nonpassing plane waves.

In order to investigate directly the transmission properties of the injected plane waves in the nonlinear periodic superlattice, we iterate numerically the discrete nonlinear equation of Eq. (2). For the initial condition $[u_0, u_1] = [1, \exp(ik)]$ we compute the transmitted wave amplitude T for a superlattice with 10^4 nonlinear planes for different nonlinearity parameter λ and wave number k . In Fig. 3 we plot the transmission coefficient $t=|T|^2$ as a function of the input wave number k for various nonlinearity values λ . There are clear transmission gaps whose width (in k space) depends on λ . We note that with increasing λ the width of each gap increases while in addition more gaps in the range between two gaps develop. This process of gap creating starts in the low energy range and extends with further increased λ also to the high energy region. Finally, above critical λ values neighboring gaps merge leading to a cancellation of transparency.

In Fig. 4 we plot the injected amplitudes for the linear ($\lambda=0$) and nonlinear ($\lambda \neq 0$) cases as a function of the wave number k . We note that the typical linear band gaps [dark areas in Fig. 4(a)] become exceedingly complicated when nonlinearity becomes nonzero [hatched region in Fig. 4(b)]. A region was considered transmitting whenever the transmission coefficient was different from zero. In particular, we observe the occurrence of new gaps in previously perfectly transmitting regions. Furthermore, the width of the passing regions (white regions) shrinks with increasing injected wave energy. The diagram was obtained by taking a grid of 500 values of k and 250 values $|R_0|$ and iterating Eq. (2) on each individual point of the grid over the $N=10^4$ sites.

The “band structure” shown in Fig. 4 can be obtained directly from the tight-binding-like Eq. (2). In the linear case, i.e., for $\lambda=0$, the allowed propagating band states are obtained from the well-known Kronig–Penney condition

$$\left| \cos(k) + \frac{1}{2} \alpha \frac{\sin(k)}{k} \right| \leq 1. \quad (5)$$

In the nonlinear Kronig–Penney case, on the other hand, this condition for propagation gets modified leading to

$$\left| \cos(k) + \frac{1}{2} \alpha (1 + \lambda |u|^2) \frac{\sin(k)}{k} \right| \leq 1. \quad (6)$$

The explicit occurrence of the wave intensity in the inequality (6) causes a broadening of the instability regions and also produces new instability tongues in the region of former allowed bands for λ values above a critical one. Furthermore, merging of neighboring instability regions is possible leading to an enhanced parameter instability.

The results we presented for the least transmitting case of $\alpha > 0$ are also sustained qualitatively in the more transmitting and physically relevant for dielectrics case of $\alpha < 0$. In general, the presence of nonlinearity in the dielectric superlattice planes alters substantially the transmission properties of the waves. In particular, when the nonlinear coefficient λ is increased new nontransmitting regions appear adjacent to the regular instability regions. Consequently, for a given wave number k , an appropriate change of the input power of the wave (corresponding to a change in λ) can switch the wave from a transmitting to a nontransmitting region. Is it then possible by a simple amplitude modulation of the incoming wave to transmit binary information to the other side of the transmission line in the forms of zeros (non transmitting region) and ones (transmitting region). Since this transmitting capability depends critically on the properties of the nontransmitting regions, further study of these regions under the nonscalar wave approximation is currently under way.

We acknowledge partial support from the US Air Force Phillips Labs.

¹S. John, Phys. Rev. Lett. **53**, 2169 (1984).

²S. John, Phys. Rev. Lett. **58**, 2486 (1987).

³E. Yablonovitch, Phys. Lett. **58**, 2059 (1987).

⁴S. John and R. Rangarajan, Phys. Rev. B **38**, 10101 (1988).

⁵K. M. Ho, C. T. Chan, and C. M. Soukoulis, Phys. Rev. Lett. **65**, 3152 (1990).

⁶M. Sigalas, C. M. Soukoulis, E. N. Economou, C. T. Chan, and K. M. Ho, Phys. Rev. B **48**, 121 (1993).

⁷W. Chen and D. L. Mills, Phys. Rev. Lett. **58**, 160 (1987); Phys. Rev. B **36**, 6269 (1987).

⁸M. I. Molina, W. D. Deering, and G. P. Tsironis, Physica D **66**, 135 (1993).

⁹J. Bellisard, A. Formoso, R. Lima, and D. Testard, Phys. Rev. B **26**, 3024 (1982).

¹⁰D. Würzt, M. P. Soerensen, and T. Schneider, Helvetica Physica Acta **61**, 345 (1988).

¹¹D. Hennig, H. Gabriel, G. P. Tsironis, and M. I. Molina (unpublished).